ELSEVIER

Cell Biology International 28 (2004) 699–708

Cell Biology International

www.elsevier.com/locate/cellbi

Structure, isolation, composition and reconstitution of the neuronal fusion pore

Won Jin Cho[a,1], Aleksandar Jeremic[a,1], Kathy T. Rognlien[a], Mzia G. Zhvania[b], Ilia Lazrishvili[b], Bikashvili Tamar[b], Bhanu P. Jena[a,*]

[a] *Department of Physiology, Wayne State University School of Medicine, 5245 Scott Hall, 540 E Canfield, Detroit, MI 48201, USA*
[b] *Section of Neuroanatomy, Institute of Physiology, Georgian Academy of Sciences, Tbilisi 380060, Georgia*

Received 8 July 2004; revised 11 July 2004; accepted 15 July 2004

Abstract

Neuronal communication is dependent on the fusion of 40–50 nm in diameter synaptic vesicles containing neurotransmitters, at the presynaptic membrane. Here we report for the first time at 5–8 Å resolution, the presence of 8–10 nm in diameter cup-shaped neuronal fusion pores or porosomes at the presynaptic membrane, where synaptic vesicles dock and fuse to release neurotransmitters. The structure, isolation, composition, and functional reconstitution of porosomes present at the nerve terminal are described. These findings reveal the molecular mechanism of neurotransmitter release at the presynaptic membrane of nerve terminals.

Keywords: Fusion pore; Neuron; AFM; SNAREs; Reconstitution

1. Introduction

In the past decade, a supramolecular structure called fusion pore or porosome has been identified at the cell plasma membrane of exocrine and neuroendocrine cells, where membrane-bound vesicles transiently dock and fuse to expel their contents during secretion (Cho et al., 2002a,b,c; Jena et al., 2003; Jena, 2004; Jeremic et al., 2003; Schneider et al., 1997). The structure, composition, and reconstitution of this secretory machinery in the exocrine pancreas are well advanced (Cho et al., 2002a; Jena et al., 2003; Jeremic et al., 2003). However, the molecular mechanism of docking and fusion of synaptic vesicles at the presynaptic membrane is unclear. In this study, we used high resolution transmission electron microscopy (TEM) and atomic force microscopy (AFM) to identify and examine neuronal porosomes of the presynaptic membrane at 5–8 Å resolution. To understand the dynamics of synaptic vesicles at porosomes, isolated synaptosomal membrane preparations were imaged using the AFM. Porosomes were isolated and their composition determined immunochemically. Isolated porosomes were then reconstituted into lipid bilayers for both structural and functional analysis using AFM and an electrophysiological bilayer apparatus (Jeremic et al., 2003; Cho et al., 2002c). Continuous capacitance measurements of the reconstituted bilayer membrane were recorded following exposure to synaptic vesicles.

* Corresponding author. Tel.: +1 313 577 1532; fax: +1 313 993 4177.
E-mail address: bjena@med.wayne.edu (B.P. Jena).
[1] Won Jin Cho and Aleksandar Jeremic contributed equally to this work.

1065-6995/$ - see front matter © 2004 International Federation for Cell Biology. Published by Elsevier Ltd. All rights reserved.
doi:10.1016/j.cellbi.2004.07.004

2. Materials and methods

2.1. Electron microscopy

Rat brain was perfused with normal saline solution, followed by phosphate buffer (pH 7.4) containing 2.5% glutaraldehyde. After perfusion, the brain was carefully removed and diced into 1 mm^3 pieces. The pieces of brain tissue were post-fixed in phosphate buffer containing 1.5% osmium tetroxide, dehydrated in graded ethanol and acetone, and embedded in araldite. Tissue blocks were appropriately trimmed and the 40–50 nm sections obtained were stained with lead citrate, and examined under a JEOL JEM-100C transmission electron microscope.

2.2. Isolation of synaptosomes, synaptosomal membrane and synaptic vesicles

Synaptosomes, synaptosomal membrane and synaptic vesicles were prepared from rat brains (Jeong et al., 1998; Thoidis et al., 1998). Whole brain from Sprague–Dawley rats (100–150 g) was isolated and placed in an ice-cold buffered sucrose solution (5 mM Hepes pH 7.4, 0.32 M sucrose) supplemented with protease inhibitor cocktail (Sigma, St. Louis, MO) and homogenized using Teflon–glass homogenizer (8–10 strokes). The total homogenate was centrifuged for 3 min at 2500 × *g*. The supernatant fraction was further centrifuged for 15 min at 14,500 × *g*, and the resultant pellet was resuspended in buffered sucrose solution, which was loaded onto 3–10–23% Percoll gradients. After centrifugation at 28,000 × *g* for 6 min, the enriched synaptosomal fraction was collected at the 10–23% Percoll gradient interface. To isolate synaptic vesicles and synaptosomal membrane (Thoidis et al., 1998), isolated synaptosomes were diluted with nine volumes of ice-cold H_2O (hypotonic lysis of synaptosomes to release synaptic vesicles) and immediately homogenized with three strokes in Dounce homogenizer, followed by a 30 min incubation on ice. The homogenate was centrifuged for 20 min at 25,500 × *g*, and the resultant pellet (enriched synaptosomal membrane preparation) and supernatant (enriched synaptic vesicles preparation) were used in our studies.

2.3. Preparation of lipid bilayer and electrophysiological measurements

Lipid bilayers were prepared using brain phosphatidylethanolamine (PE) and phosphatidylcholine (PC), and dioleoylphosphatidylcholine (DOPC), and dioleoylphosphatidylserine (DOPS) obtained from Avanti Lipids (Alabaster, AL). A suspension of PE:PC in a ratio of 7:3, and at a concentration of 10 mg/ml was prepared. Lipid suspension, 100 μl, was dried under nitrogen gas and resuspended in 50 μl decane. To reconstitute the bilayer with neuronal porosomes, the SNAP-25 immunoisolates obtained from nonionic-detergent-solubilized synaptosomal membrane preparations was added to the lipid suspension and brushed onto a 200 μm hole in the bilayer chamber until a stable bilayer with a capacitance between 100 and 250 pF was obtained.

2.4. Preparation of lipid membrane on mica and porosome reconstitution

To prepare lipid membrane on mica for AFM studies, freshly cleaved mica disks were placed in a fluid chamber. Bilayer bath solution (200 μl), containing 140 mM NaCl, 10 mM HEPES, and 1 mM $CaCl_2$, was placed at the center of the cleaved mica disk. Brain lipid vesicles (10 μl) were added to the above bath solution. The mixture was then allowed to incubate for 60 min at room temperature, before washing (×10), using 100 μl bath solution/wash. The lipid membrane on mica was imaged by the AFM before and after the addition of immunoisolated porosomes.

2.5. Atomic force microscopy

Isolated synaptosomes or synaptosomal membrane preparations in PBS, pH 7.5, were imaged with the AFM (BioScope III, Digital Instruments, Santa Barbara, CA) using both contact and ''tapping'' modes. All images presented in this study were obtained in the tapping mode in fluid, using silicon nitride tips with a spring constant of 0.06 N/m, and an imaging force of $<$200 pN. To obtain high resolution images, imaging force of 300–500 pN was used. Images were obtained at line frequencies of 1.98 Hz, with 512 lines per image, and constant image gains. Topographical dimensions of porosomes and synaptic vesicles at the presynaptic membrane were analyzed using the software NanoScope IIIa version 4.43r8 supplied by Digital Instruments.

2.6. Immunoprecipitation, Sypro protein staining and Western blot analysis

To isolate the neuronal fusion pore or porosome complex, SNAP-25 specific antibody conjugated to protein A-sepharose was used. One gram of total rat brain homogenate solubilized in Triton/Lubrol solubilization buffer (0.5% Lubrol; 1 mM benzamidine; 5 mM Mg-ATP; 5 mM EDTA; 0.5% Triton X-100, in PBS) supplemented with protease inhibitor mix (Sigma, St. Louis, MO) was used. SNAP-25 antibody conjugated to the protein A-sepharose was incubated with the solubilized homogenate for 1 h at room temperature followed by washing with wash buffer (500 mM NaCl,

10 mM Tris, 2 mM EDTA, pH 7.5). The immunoprecipitated sample attached to the immunosepharose beads was eluted using low pH buffer to obtain the porosome complex. Immunoblot analysis was performed on brain fractions and the immunoisolates. Protein in the fractions was estimated by the Bradford method (Bradford, 1976). All fractions were boiled in Laemmli reducing sample preparation buffer (Laemmli, 1970) for 5 min, cooled, and used for SDS-PAGE. Proteins were resolved in a 12.5% SDS-PAGE and electrotransferred to 0.2 mm thick nitrocellulose sheets for immunoblot analysis using specific antibodies. Immunoblot analysis was performed using specific antibodies to actin, VAMP-2 and syntaxin-1 (Alomone Labs, Jerusalem, Israel), vimentin (Sigma, St. Louis, MO), NSF (Exalpha Biologicals, Boston, MA), Gαo, CLC-3 and Ca^{2+}-P/Q (Santa Cruz Biotechnology, Santa Cruz, CA). Anti-synaptotagmin-1 and SV2 were a gift from R. Jahn. The nitrocellulose membrane was incubated for 1 h at room temperature in blocking buffer (5% non-fat milk in PBS containing 0.1% Triton X-100 and 0.02% NaN_3), and immunoblotted for 2 h at room temperature with the primary antibody. The immunoblotted nitrocellulose sheets were washed in PBS containing 0.1% Triton X-100 and 0.02% NaN_3 and were incubated for 1 h at room temperature in horseradish peroxidase-conjugated secondary antibody at a dilution of 1:2000 in blocking buffer. The immunoblots were then washed in the PBS buffer, processed for enhanced chemiluminescence and photographed using a Kodak Image Station 414. To identify the different protein bands resolved by SDS-PAGE, fluorescent Sypro Ruby (Molecular Probes, Eugene, OR) protein staining of the gels was performed. Stained bands were visualized by using the UV illuminator and a 590 nm bandpass emission filter of the Kodak Imager.

3. Results and discussion

To determine the sites where synaptic vesicles dock and fuse, boutons at the nerve terminal in rat brain tissue were imaged using TEM (Fig. 1a). Careful examination of the presynaptic membrane in boutons reveal the presence of 8–10 nm cup-shaped porosomes with 40–50 nm synaptic vesicles docked at its base (Fig. 1b–d). The porosomes appear to have a plug-like structure at the center. In a number of micrographs, a lone vesicle was found docked at the base of two porosomes (Fig. 1d).

To determine the structure of the porosome opening in the hydrated state in live tissue, isolated synaptosomes from brain were placed on a mica surface in physiological buffer solution, and imaged using the AFM (Fig. 1e–h). In a number of synaptosomes where the postsynaptic membrane was absent, the outer surface of the presynaptic membrane reveals the presence of porosomes in patches (Fig. 1g, yellow arrowheads). Further increase in resolution reveals in 3-D the 8–10 nm diameter porosomes as having a distinct plug at the center (Fig. 1h, green arrowhead). In Fig. 1h, the red arrowhead points to the porosome opening to the outside. As previously identified in exocrine pancreas (Cho et al., 2002a; Jena et al., 2003; Jeremic et al., 2003; Schneider et al., 1997) and in neuroendocrine cell secretion (Cho et al., 2002b,c; Jena, 2004; Jeremic et al., 2003), the porosome in neurons is demonstrated for the first time.

Similar to the isolation of porosomes from the exocrine pancreas (Jena et al., 2003; Jeremic et al., 2003), neuronal porosomes were immunoisolated from detergent-solubilized synaptosome preparations, using a SNAP-25 specific antibody. Electrophoretic resolution of the immunoisolates revealed the presence of 12 distinct protein bands, as determined by Sypro protein staining of the resolved complex (Fig. 2a). Further, electrotransfer of the resolved porosomal complex onto nitrocellulose membrane, followed by immunoblot analysis using various antibodies, revealed nine proteins. In agreement with earlier findings (Faigle et al., 2000; Jena et al., 2003; Jeremic et al., 2003; Nakano et al., 2001; Ohyama et al., 2001; Prekereis and Terrian, 1997), SNAP-25, the P/Q-type calcium channel, actin, syntaxin-1, synaptotagmin-1, vimentin, the *N*-ethylmaleimide-sensitive factor (NSF) (Jena et al., 2003; Jeremic et al., 2003; Rothman, 1994), the chloride channel CLC-3 and the alpha subunit of the heterotrimeric GTP-binding G_o, were identified as constituent parts of the complex. To test whether the complete porosome complex was immunoisolated, the immunoisolate preparation was reconstituted into lipid membrane prepared using brain dioleoylphosphatidylcholine (DOPC) and dioleoylphosphatidylserine (DOPS) in a ratio of 7:3. At low resolution, the AFM showed the immunoisolates to arrange in L- or V-shaped structures (Fig. 2b, red arrowheads), which at higher resolution demonstrated the presence of porosomes in patches (Fig. 2c, d, green arrowheads), similar to what is observed at the presynaptic membrane in intact synaptosomes (Fig. 1g, yellow arrowheads). Further imaging of the reconstituted immunoisolate at greater resolutions using the AFM demonstrated the presence of 8–10 nm porosomes (Fig. 2e). As observed in electron (Fig. 1b–d) and AFM micrographs (Fig. 1h) of the presynaptic membrane in synaptosomes, the immunoisolated and lipid-reconstituted porosome possess an approximately 2 nm diameter central plug. These studies confirm the complete isolation and structural reconstitution of the neuronal porosome in artificial lipid bilayers.

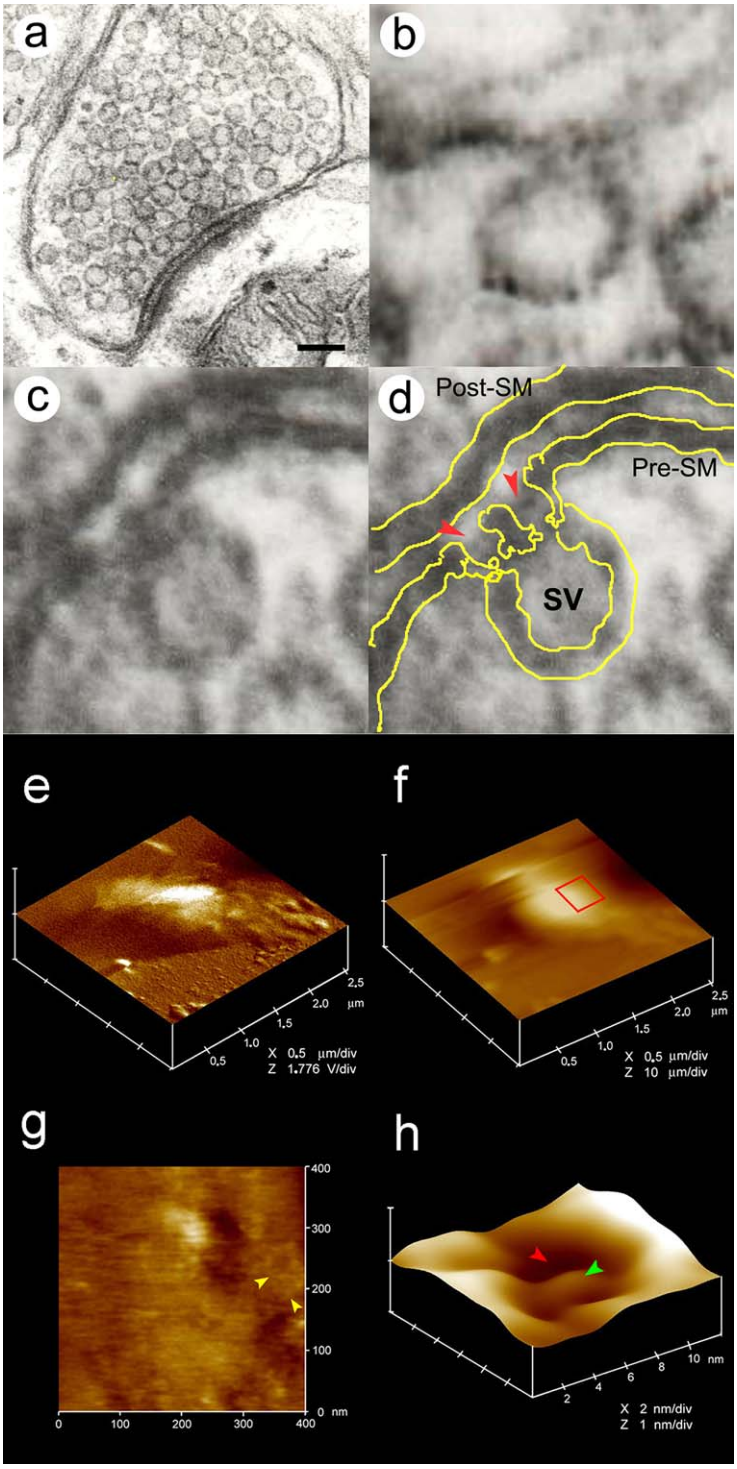

Fig. 1. Fusion pores or porosomes at the presynaptic membrane of synaptosomes in brain tissue. (a) Electron micrograph of a single synaptosome full of 40–50 nm synaptic vesicles, and with intact presynaptic (Pre-SM) and postsynaptic membranes (Post-SM). Bar = 100 nm. (b–d) At higher magnification, 8–10 nm diameter porosomes (red arrowheads) with 40 nm synaptic vesicles (SV) docked at the porosome base, are observed at the presynaptic membrane. (e, f) Atomic force micrographs of isolated rat brain synaptosomal preparations in PBS (Jeong et al., 1998; Thoidis et al., 1998). An area (red outline) of the synaptosome devoid of the postsynaptic membrane was imaged at higher resolution, (g) revealing patches of porosomes (yellow arrowheads). Further increase in resolution reveals several 8–10 nm porosomes within each patch. (h) A single porosome with a central plug (green arrowhead) is shown in 3-D.

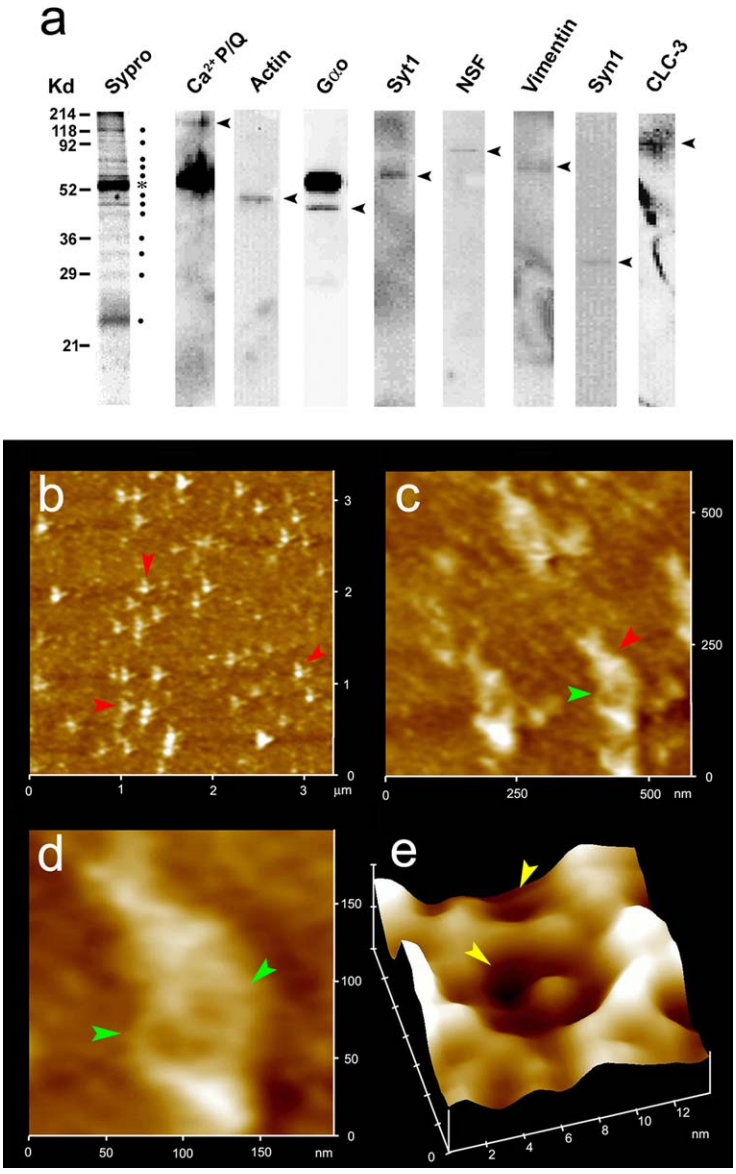

Fig. 2. Composition of the neuronal porosome and its reconstitution in lipid membrane. (a) Proteins immunoisolated from detergent-solubilized synaptosomal membrane preparation, using a SNAP-25 specific antibody. Immunoisolates when resolved by SDS-PAGE, and the resolved proteins in the gel stained using Sypro dye, reveals 12 specific bands (●), suggesting the presence of at least 12 proteins in the complex, not including the heavy chain (*) of the SNAP-25 antibody. When the resolved proteins were electrotransferred to nitrocellulose membrane and probed with various antibodies, calcium channel P/Q, actin, Gαo, syntaxin-1 (Syn1), synaptotagmin-1 (Syt1), NSF, vimentin, and the chloride channel CLC-3 were identified (Bradford, 1976; Laemmli, 1970). (b–e) Atomic force micrographs at different resolution of the reconstituted immunoisolate in lipid membrane. (b) At low magnification, the immunoisolated complex arrange in L- or V-shaped structures (red arrowheads). (c, d) Within the V-shaped structures, patches (green arrowheads) of porosomes are found. (e) Each reconstituted porosome is almost identical to the porosome observed in intact synaptosomes. The central plug is clearly seen. This AFM micrograph demonstrates the presence of two porosomes (yellow arrowhead), although only half of the second porosome is in the picture.

In order to understand the structure of the porosome at the cytosolic side of the presynaptic membrane, isolated synaptosomal membrane preparations were imaged by the AFM. These studies reveal the architecture of the cytosolic part of porosomes. In synaptosomes, 40–50 nm synaptic vesicles are arranged in ribbons, as seen in the electron micrographs (longitudinal section, Fig. 3a, or in cross-section Fig. 3b). Similarly, when the cytosolic domain of isolated synaptosomal membrane preparations was analyzed by the AFM, 40–50 nm synaptic vesicles were also found to be arranged in ribbons (Fig. 3c, d), thus confirming our EM observations. On close examination (Fig. 3d–f) of the docked synaptic vesicles (blue arrowheads), we observed that synaptic vesicles were attached to the base of the 8–10 nm porosomes (red arrowheads). It was

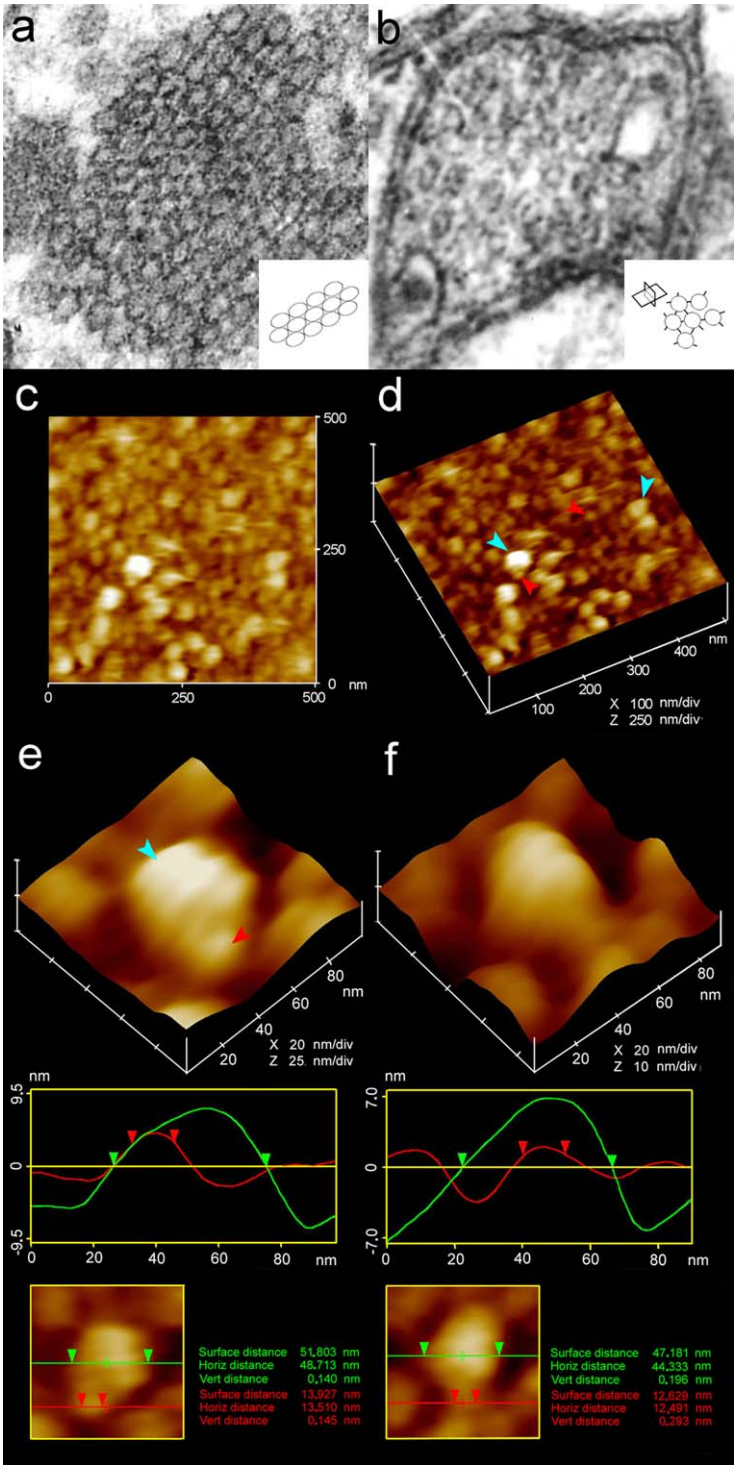

Fig. 3. Arrangement of synaptic vesicles and porosomes within the synaptosome. (a) Electron micrograph of rat brain synaptosome demonstrating the ribbon-like arrangement (inset) of 40–50 nm synaptic vesicles. (b) Cross-section of such a ribbon (inset) reveals the interaction between the synaptic vesicles. (c, d) Examination of the presynaptic membrane from the cytosolic side (inside out) using AFM, confirmed such a ribbon arrangement of docked synaptic vesicles (blue arrowheads) at porosomes (red arrowheads). Bare porosomes (lacking docked synaptic vesicles) were also seen. The AFM micrograph in c is a 2-D image and in d, a 3-D image. (e, f) AFM micrograph of a docked synaptic vesicle at a porosome. During imaging using the AFM, the interaction of the cantilever tip with the sample sometimes resulted in pushing away the docked synaptic vesicle, enough to expose the porosome lying beneath. AFM section analysis further reveals the size of synaptic vesicles (green section line and arrowheads) and porosomes (red section line and arrowheads).

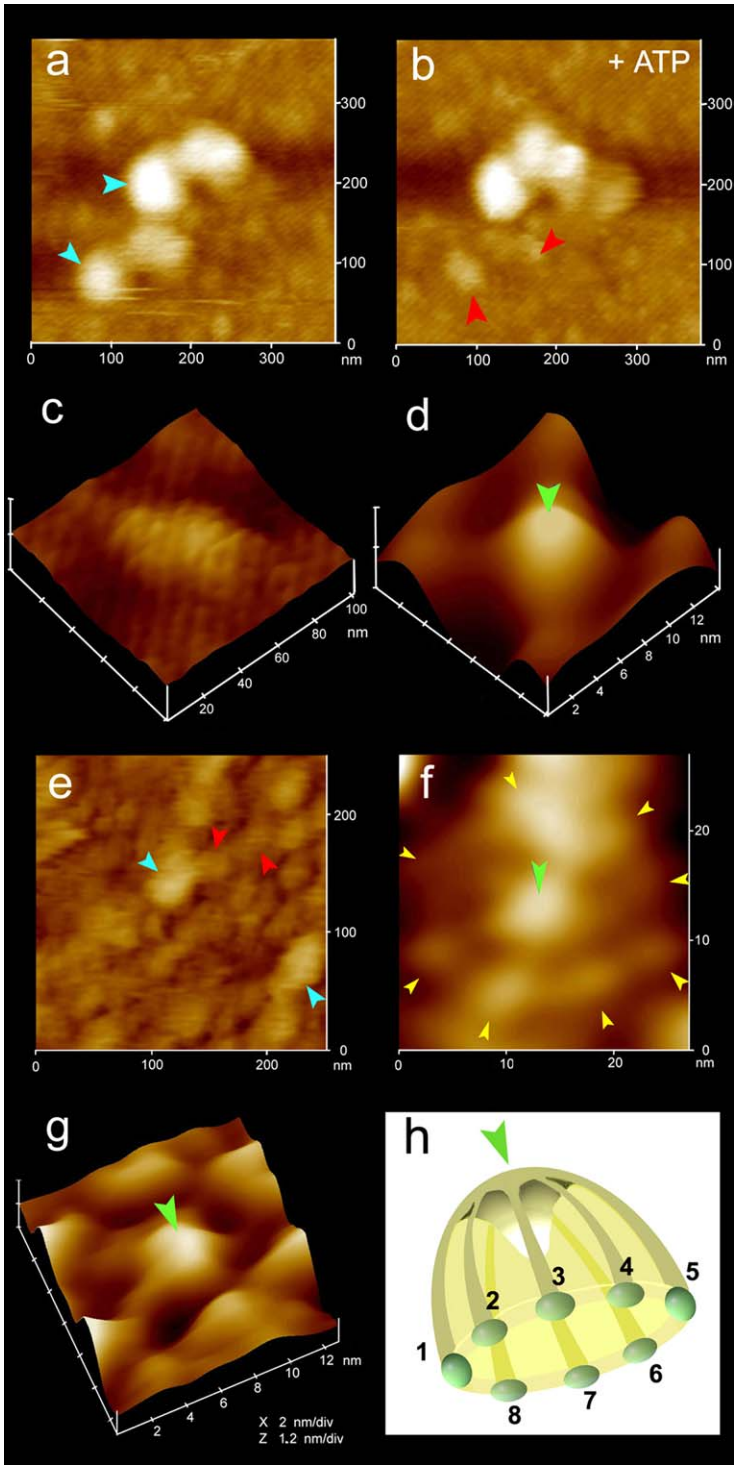

Fig. 4. AFM micrographs revealing the dynamics of docked synaptic vesicles at porosomes and the porosome architecture in greater detail. (a) AFM micrograph of five docked synaptic vesicles at porosomes. (b) Addition of 50 μM ATP, dislodges two synaptic vesicles at the lower left, and exposing the porosome patches (red arrowheads). This also reveals that a single synaptic vesicle may dock at more than one porosome complex (and as also observed in electron micrographs in Fig. 1c, d). (c–g) AFM micrographs obtained at higher imaging forces (300–500 pN rather than <200 pN) reveal porosomes architecture at greater detail. (c) AFM micrograph of one of the porosome patches where a synaptic vesicle was docked prior to ATP exposure. (d) Base of a single porosome. (e) High force AFM micrograph of the cytosolic face of the presynaptic membrane, demonstrating the ribbon arrangement of porosome patches (red arrowhead) and docked synaptic vesicles (blue arrowheads). Note how the spherical synaptic vesicles are compressed and flattened at higher imaging forces. (f, g) At such higher imaging forces, porosomes reveal the presence of eight globular structures (yellow arrowhead) surrounding a central plug (green arrowhead), as demonstrated in the (h) schematic diagram.

possible to see both the porosome and the attached synaptic vesicle, since while imaging with the AFM, synaptic vesicles were slightly pushed away from their docked sites to reveal the porosome lying beneath (Fig. 3c–f). Additionally, bare porosomes with no synaptic vesicles attached, were also found at the cytosolic side of synaptosomal membrane preparations (Fig. 3d).

In the presence of calcium (Jeremic et al., 2004), target membrane proteins, SNAP-25 and syntaxin (t-SNARE) and secretory vesicle-associated membrane protein (v-SNARE) are a part of the conserved protein complex involved in fusion of opposing bilayers (Weber et al., 1998). NSF is an ATPase that is thought to disassemble the t-/v-SNARE complex in the presence of ATP (Jeong et al., 1998; Rothman, 1994). To test this hypothesis, and to further confirm and determine the porosome morphology, synaptosomal membrane preparations with docked synaptic vesicles were imaged using the AFM in the presence and absence of ATP (Fig. 4a). As hypothesized, addition of 50 μM ATP resulted in t-/v-SNARE disassembly and the release of docked vesicles (blue arrowhead) at the porosome patch (Fig. 4b, c, red arrowhead). At higher resolution, the base of the porosome is clearly revealed (Fig. 4d). At increased imaging forces (300–500 pN instead of <200 pN), porosome patches (Fig. 4e, red arrowhead) and individual porosomes (Fig. 4f, g) were further defined in greater structural detail. At 5–8 Å resolution, eight peripheral knobs at the porosomal opening (Fig. 4f–h, yellow arrowheads) and a central plug (green arrowhead) at the base, were revealed. These studies provide again another direct demonstration of synaptic vesicle docking at these sites, confirming them to be porosomes, where synaptic vesicles dock and transiently fuse to release neurotransmitters (Aravanis et al., 2003). Hence, synaptic vesicles are able to fuse transiently and successively at porosomes in the presynaptic membrane without loss of identity, as reported by Aravanis et al. (2003).

To assess the functionality of the reconstituted porosome preparations (Figs. 2e, 5a), an electrophysiological bilayer setup was used (Fig. 5b). Membrane capacitance was continually monitored throughout

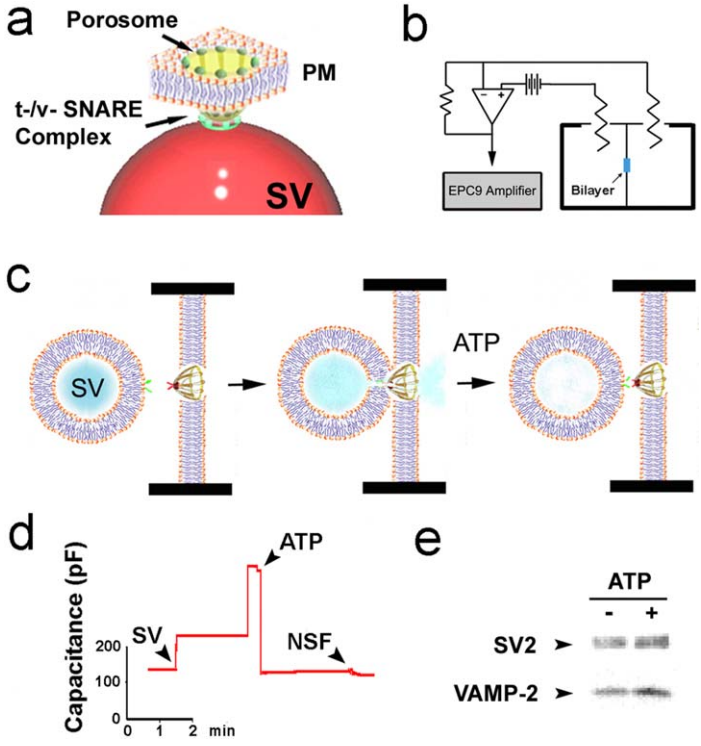

Fig. 5. Functional reconstitution of immunoisolated porosomes. (a) Schematic representation of a porosome at the presynaptic membrane, with a docked synaptic vesicle at its base. (b) Schematic drawing of an EPC9 electrophysiological bilayers apparatus, to continually monitor changes in the capacitance of porosome-reconstituted membrane, when synaptic vesicles are introduced into the *cis* bilayers chamber followed by ATP and purified recombinant NSF protein. (c) Schematic representation of synaptic vesicle (SV) docking at the base of a porosome, fusing to release its contents, and disengaging in the presence of ATP. (d) Capacitance measurements of porosome-reconstituted bilayers support the experiment in Fig. 4b and the schematic diagram in c. Exposure of the reconstituted bilayers to SVs results in a dramatic increase in membrane capacitance, which drops to baseline following exposure to 50 μM ATP. Recombinant NSF has no further effect ($n = 6$). (e) Exposure of isolated synaptosomal membrane preparations to 50 μM ATP results in the release of SVs from the membrane into the incubation medium, as demonstrated by immunoblot analysis of the incubating medium using the SV-specific protein antibodies, SV2 and VAMP-2.

these experiments. Following reconstitution of the bilayer membrane with porosomes, isolated synaptic vesicles were added to the *cis* compartment of the bilayer chamber. A large number of synaptic vesicles fused at the bilayer, as demonstrated by the significant stepwise increases in the membrane capacitance (Fig. 5c, d). As expected from the results in Fig. 4b, addition of 50 μM ATP allowed t-/v-SNARE disassembly and the release of docked vesicles, resulting in the return of the bilayers membrane capacitance to resting levels (Fig. 5c, d). Addition of recombinant NSF had no further effect on membrane capacitance. Thus, the associated NSF (Fig. 2a) at the t-/v-SNARE complex is adequate for complete disassembly of the SNARE complex for release of synaptic vesicles following transient fusion and the completion of a round of neurotransmitter release. To assess biochemically the release of docked synaptic vesicles following ATP treatment, synaptosomal membrane preparations were exposed to 50 μM ATP, and the supernatant fraction was assessed for synaptic vesicles by monitoring levels of the synaptic vesicle proteins SV2 and VAMP-2 (Fig. 5e). Our study demonstrates that both SV2 and VAMP-2 proteins are enriched in supernatant fractions following exposure of isolated synaptosomal membrane to ATP (Fig. 5e). Thus, AFM, electrophysiological measurements, and immunoanalysis, confirmed the dissociation of porosome-docked synaptic vesicles following ATP exposure. As previously suggested (Jena, 1997, 2002), such a mechanism may allow for the multiple transient docking-fusion and release cycles that synaptic vesicles may undergo during neurotransmission, without loss of vesicle identity and integrity (Aravanis et al., 2003).

Due to new technological developments resulting in improved instrumentation and refined experimental procedures, we were able in this study for the first time to identify and examine at 5–8 Å resolution the fusion pore or porosomes in neurons. The neuronal porosome, although an order of magnitude smaller than those in the exocrine pancreas or in neuroendocrine cells, possess many similarities both in structure and composition. Thus, nature has designed the porosome as a general secretory machine, but has fine tuned it to suite various secretory processes in different cells; porosome size may reflect such fine tuning. It is well known that smaller vesicles fuse more efficiently than larger ones (Ohki, 1984; Wilschut et al., 1981), and hence the curvature of both the secretory vesicle and the porosome base would dictate the efficacy and potency of vesicle fusion at the cell plasma membrane. For example, neurons being fast secretory cells, possess small (40–50 nm) secretory vesicles and porosome bases (2–4 nm) for rapid and efficient fusion. In contrast, a slow secretory cell like the exocrine pancreas possesses larger secretory vesicles (1000 nm diameter) that fuse at porosomes that have bases measuring 20–30 nm diameter.

Acknowledgements

We thank D.A. Walz for critically reading the manuscript and for suggestions. This work was supported by NIH grants DK56212 and NS39918 (B.P.J.).

References

Aravanis AM, Pyle JL, Tsien RW. Single synaptic vesicles fusing transiently and successively without loss of identity. Nature 2003; 423:643–7.

Bradford MM. A rapid and sensitive method for the quantitation of microgram quantities of protein utilizing the principle of protein dye binding. Anal Biochem 1976;72:248–54.

Cho S-J, Quinn AS, Stromer MH, Dash S, Cho J, Taatjes DJ, et al. Structure and dynamics of the fusion pore in live cells. Cell Biol Int 2002a;26:35–42.

Cho S-J, Jeftinija K, Glavaski S, Jeftinija S, Jena BP, Anderson LL. Structure and dynamics of the fusion pores in live GH-secreting cells revealed using atomic force microscopy. Endocrinology 2002b;143:1144–8.

Cho S-J, Wakade A, Pappas GD, Jena BP. New structure involved in transient membrane fusion and exocytosis. Ann N Y Acad Sci 2002c;971:254–6.

Faigle W, Colucci-Guyon E, Louvard D, Amigorena S, Galli T. Vimentin filaments in fibroblasts are a reservoir for SNAP-23, a component of the membrane fusion machinery. Mol Biol Cell 2000;11:3485–94.

Jena BP. Discovery of the porosome: revealing the molecular mechanism of secretion and membrane fusion in cells. J Cell Mol Med 2004;8:1–21.

Jena BP, Cho SJ, Jeremic A, Stromer MH, Abu-Hamdah R. Structure and composition of the fusion pore. Biophys J 2003;84: 1337–43.

Jena BP. Exocytotic fusion: total or transient? Cell Biol Int 1997;21: 257–9.

Jena BP. Fusion pores in live cells. News Physiol Sci 2002;17:219–22.

Jeong E-H, Webster P, Khuong CQ, Sattar AA, Satchi M, Jena BP. The native membrane fusion machinery in cells. Cell Biol Int 1998; 22:657–70.

Jeremic A, Kelly M, Cho JA, Cho SJ, Horber JK, Jena BP. Calcium drives fusion of SNARE-apposed bilayers. Cell Biol Int 2004;28: 19–31.

Jeremic A, Kelly M, Cho SJ, Stromer MH, Jena BP. Reconstituted fusion pore. Biophys J 2003;85:2035–43.

Laemmli UK. Cleavage of structural proteins during the assembly of the head of bacteriophage T4. Nature 1970;227:680–5.

Nakano M, Nogami S, Sato S, Terano A, Shirataki H. Interaction of syntaxin with α-fodrin, a major component of the submembranous cytoskeleton. Biochem Biophys Res Commun 2001;288: 468–75.

Ohki S. Effects of divalent cations, temperature, osmotic pressure gradient, and vesicle curvature on phosphatidylserine vesicle fusion. J Memb Biol 1984;77:265–75.

Ohyama A, Komiya Y, Igarashi M. Globular tail of myosin-V is bound to vamp/synaptobrevin. Biochem Biophys Res Commun 2001;280:988–91.

Prekereis R, Terrian DM. Brain myosin V is a synaptic vesicle-associated motor protein: evidence for a Ca^{+2}-dependent interaction with the synaptobrevin–synaptophysin complex. J Cell Biol 1997;137:1589–601.

Rothman JE. Mechanism of intracellular protein transport. Nature 1994;372:55–63.

Schneider SW, Sritharan KC, Geibel JP, Oberleithner H, Jena BP. Surface dynamics in living acinar cells imaged by atomic force microscopy: identification of plasma membrane structures involved in exocytosis. Proc Natl Acad Sci U S A 1997;94:316–21.

Thoidis G, Chen P, Pushkin AV, Vallega G, Leeman SE, Fine RE, et al. Two distinct populations of synaptic-like vesicles from rat brain. Proc Natl Acad Sci U S A 1998;95:183–8.

Weber T, Zemelman BV, McNew JA, Westerman B, Gmachl M, Parlati F, et al. SNAREpins: minimal machinery for membrane fusion. Cell 1998;92:759–72.

Wilschut J, Duzgunes N, Papahadjopoulos D. Calcium/magnesium specificity in membrane fusion: kinetics of aggregation and fusion of phosphatidylserine vesicles and the role of bilayers curvature. Biochemistry 1981;20:3126–33.